J Mater Sci: Mater Electron (2020) 31:16609–16615

Rapid detection of biomolecules in a dielectric modulated GaN MOSHEMT

Shaveta[1,2], H. M. Maali Ahmed[1], and Rishu Chaujar[1,*]

[1] Department of Applied Physics, Delhi Technological University, Main Bawana Road, Delhi, India
[2] Solid State Physics Laboratory, Defence Research Development Organization, Delhi, India

Received: 2 June 2020
Accepted: 8 August 2020
Published online: 31 August 2020

ABSTRACT

Biosensors are the devices that find application in almost every field nowadays. In this paper, GaN MOSHEMT based biosensor is proposed for detection of biomolecules such as ChOx, protein, streptavidin and Uricase. The effect of biomolecule species on the performance parameters of the device has been studied. It has been observed that there is a significant increase in the drain current and g_d is observed with the addition of biomolecule in the nanocavity. The electron concentration contour is studied which shows the rise of carrier concentration with biomolecule. Maximum positive shift is observed in threshold voltage for Uricase due to lowest dielectric constant. Similarly, the change in transconductance is also obtained with biomolecules. The effect of cavity dimensions on sensitivity is also studied. The maximum increase of 10% in channel potential is noted due biomolecule presence in the cavity. This device has shown good sensing and can be used for biosensing applications efficiently in addition to the high power performance of MOS-HEMTs.

1 Introdcution

The recent COVID-19 pandemic has again brought in forefront the importance of electronic biosensors in detection of biomolecules & biological warfare agents. The electronic biosensors may find applications in real time monitoring of airborne biomolecules in transport systems like aircrafts & metro rail and centrally air conditioned buildings like schools, hospitals, etc. Therefore, the need of the hour is to design and develop fast and accurate biosensors.

Biosensors use chemical reactions to detect the biochemical compounds such as antibodies, biological molecules, nucleic acids, enzymes etc. So they are widely used in many applications such as monitoring of diseases, food analysis, crime detection, environmental field monitoring, and also for the study of biomolecules interaction [1, 2].

Now a days Gallium Nitride (GaN) is emerging as one of the most promising material due to very promising properties. GaN has wide band gap of 3.4 eV and can operate at high temperature (> 300 °C) as compare to silicon, which is being used to fabricate conventional devices. Apart from this they have high electric field, polarization nature, distinctive chemical stability in the biological

Address correspondence to E-mail: chaujar.rishu@dtu.ac.in

https://doi.org/10.1007/s10854-020-04216-7

atmosphere, low level of toxicity to the living cells, and the ability to integration with other electronic devices [3–7]. AlGaN/GaN HEMT shows promising biological/chemical sensing applications due to the presence of 2DEG (Two-dimensional electron gas) at the hetero interface. Any biomolecules can get easily attached to AlGaN barrier layer that varies the surface charges at the AlGaN/GaN interface and as a counter effect channel properties are varied. So interface property [8] is very crucial parameter in determining the device functionality. So HEMT based gas sensors, mercury and chlorine ion sensors, pH sensors, DNA sensors, glucose sensor, cancer biomarker detector, terahertz sensors, strain sensors etc. have been developed [9, 10].

Extensive work has been done by various researchers on FET based biosensors for detection of various biomolecules. Schwarz et al. have reported a novel HEMT-based hybridization sensor using photochemical functionalization to detect DNA [11]. Khazanskaya et al. have reported field-effect transistor biosensor for ammonium ions and urea detection [12]. Chen et al. used Au-gated AlGaN/GaN HEMTs to detect c-erbB-2, which is a breast cancer marker [13]. Kannan reported GaN HEMT to detect pH and biomarkers for the detection of biomolecules using MOS transistor sensor [14]. Yantao et al. have invented an effective FET biosensor for Ebola Antigen detection [15]. Chung et al. demonstrated AlGaN/GaN HEMT hydrogen gas sensor at extreme environmental conditions [16]. Hu proposed AlGaN/GaN/AlN quantum-well MOS-HEMTs based on numerical simulations [17]. Recently, Seo et al. reported a field-effect transistor (FET)-based biosensing device by using graphene sheet for detecting SARS-CoV-2 in clinical samples [18].

In this paper, Simulation of GaN MOSHEMT based biosensor for detection of neutral biomolecule such as ChOx, protein, streptavidin and Uricase has been demonstrated. Although gate-all-around junctionless transistor (GAA-JLT) [19] and inversion mode MOSFETs [20] have been demonstrated in past for label-free electrochemical detection of neutral biomolecule. As compare to these devices GaN MOSHEMT devices have advantages of reduced gate leakage current density, high breakdown voltage and high electron mobility under both low and high transverse fields [21, 22]. The structure is analyzed by using dielectric modulation technique. Silvaco TCAD software is used for simulation of the structure.

Section 2 presents the device architecture and models used for simulation. Section 3 discusses the device current model used for simulation. Results including output and transfer characteristics, sensitivity and channel potential are discussed in Section 5.

2 Device architecture

Figure 1a highlights the schematic cross-section of AlGaN/GaN MOSHEMT. The structure has 1 μm thick GaN buffer layer, 1 nm AlN spacer, 20 nm oxide, 18 nm $Al_{0.20}Ga_{0.80}$ N barrier. The gate length (L_G) is 5 μm, length between source and gate (L_{SG}) is 1 μm and between gate and drain (L_{GD}) is 2 μm. The structure is passivated by thin film of Si_3N_4 layer to reduce surface states effect. The complete length and width of the device is 9 μm and 100 μm, respectively. Contact taken at the gate terminal is Schottky and at source & drain is ohmic. Initially the region below the cavity was filled with SiO_2 and later two cavities of 1.5 μm each are considered in region I and III underneath the gate electrode as shown in Fig. 1b. This region is confined on the top of AlGaN layer to induce and detect biomolecule. In this paper, neutral biomolecules like ChOx, Protein, Streptavidin and Uricase are introduced in the cavity. The dielectric constant of these biomolecules is given in Table 1.

Considered neutral biomolecules do not react with the SiO_2 interface. They only introduce the dielectric in the region and the structure is like gate-stack.

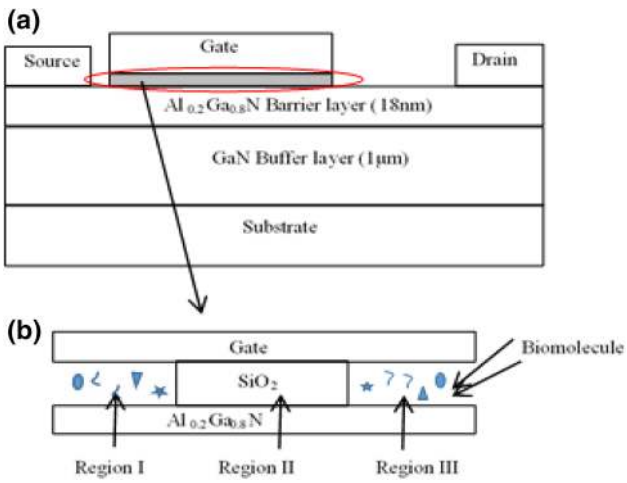

Fig. 1 **a** Schematic of AlGaN/GaN MOSHEMT with nanocavity for biomolecules. **b** Magnified view of cavity region introduced below gate region

Therefore, the presence of neutral biomolecules can be modeled by introducing material with a dielectric constant corresponding to neutral biomolecules. This approach has been calibrated with experimental results [23].

All simulations are carried out in Silvaco TCAD software. The models used are polarization model, Shockley–Read–Hall (SRH) recombination mode, field dependent drift velocity (FLDMOB) model, concentration dependent mobility (CONMOB), albrct.n and 8.85 × 10^{12} cm^{-2} of interface charges are considered at the AlGaN/GaN interface.

3 Device current model

As shown in Fig. 1b region I and III is empty cavity to be filled with biomolecule and region II is oxide layer. The capacitance for different regions is given by Eqs. (1) and (2)

$$C_{SiO_2} = \frac{\varepsilon_{SiO_2}}{t_{ox}} \tag{1}$$

$$C_{Bio} = \frac{2\varepsilon_{Bio}}{t_{Bio}} \tag{2}$$

where, ε_{SiO2}, ε_{Bio}, t_{ox} and t_{Bio} are permittivity and thickness of SiO_2 and biomolecule, respectively. The thickness of oxide and biomolecule layer is kept constant for simplicity.

The total capacitance of the region I, II and III is given by Eq. (3)

$$C_{Total} = C_{SiO_2} + C_{Bio} \tag{3}$$

Total capacitance of the MOSHEMT device is given by Eq. (4)

$$\frac{1}{C_{MOSHEMT}} = \frac{1}{C_{HEMT}} + \frac{1}{C_{total}} \tag{4}$$

where, C_{HEMT} is the capacitance of the Device [24]. The drain current for the device is given by Eq. (5) Ref.[25],

Table 1 Dielectric constant of biomolecules

Biomolecule	Permittivity
ChOx	3.5
Protein	2.5
Streptavidin	2.1
Uricase	1.5

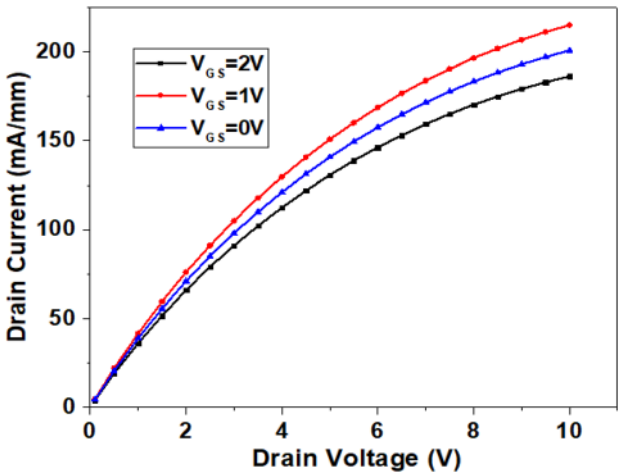

Fig. 2 Output characteristics of AlGaN/GaN MOSHEMT without biomolecules at different gate voltages

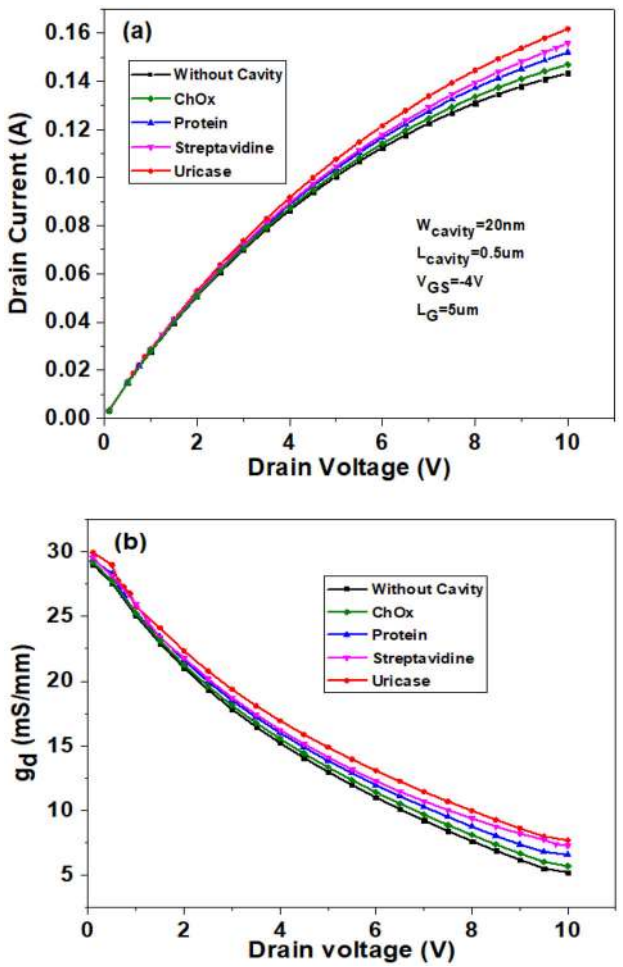

Fig. 3 **a** Output characteristics **b** g_d vs Vd of AlGaN/GaN MOSHEMT with different biomolecules introduced in the cavity

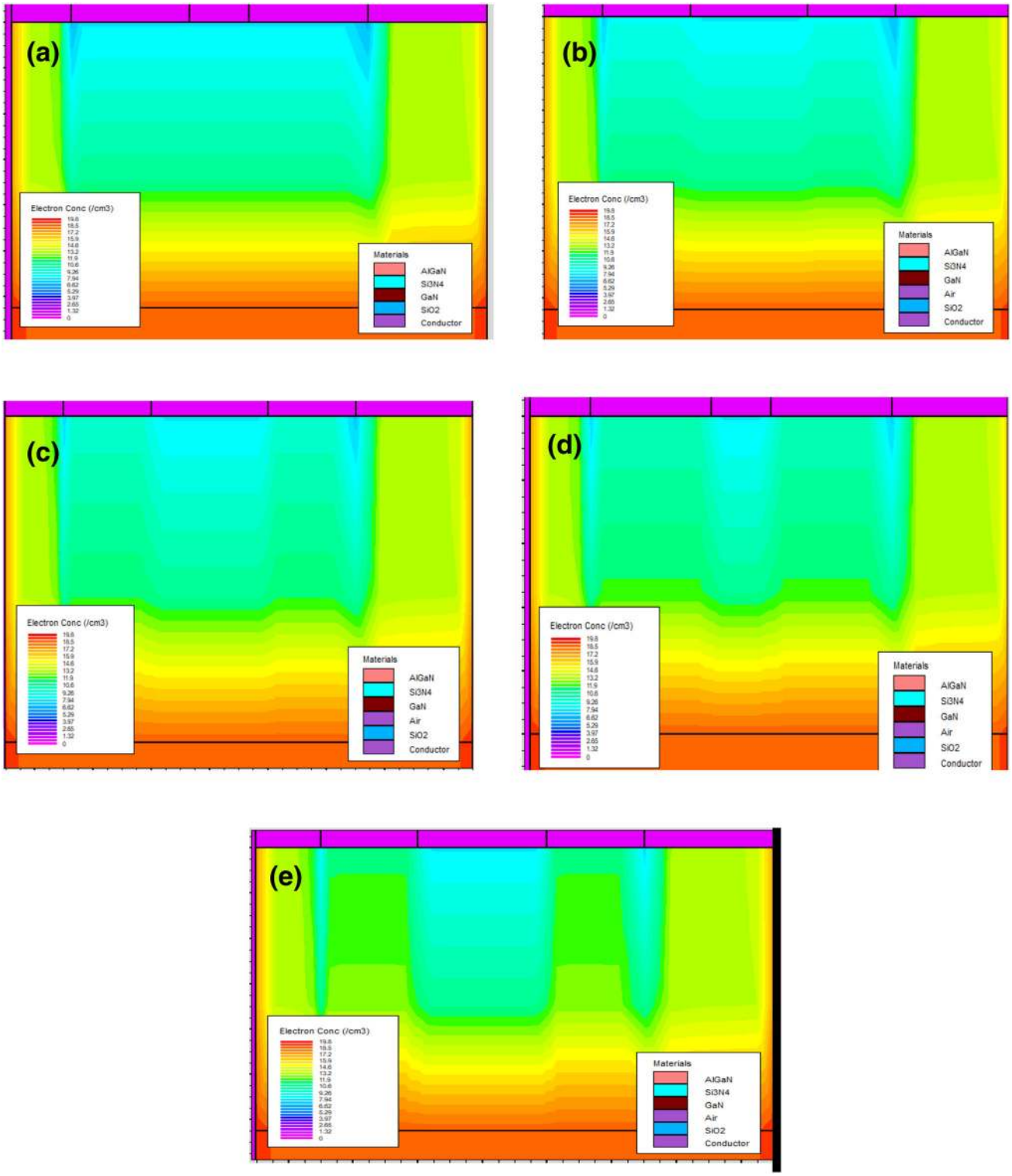

Fig. 4 Electron concentration contour (**a**) without biomolecule (**b**) ChOx (**c**) Protein (**d**) Streptavidin (**e**) Uricase

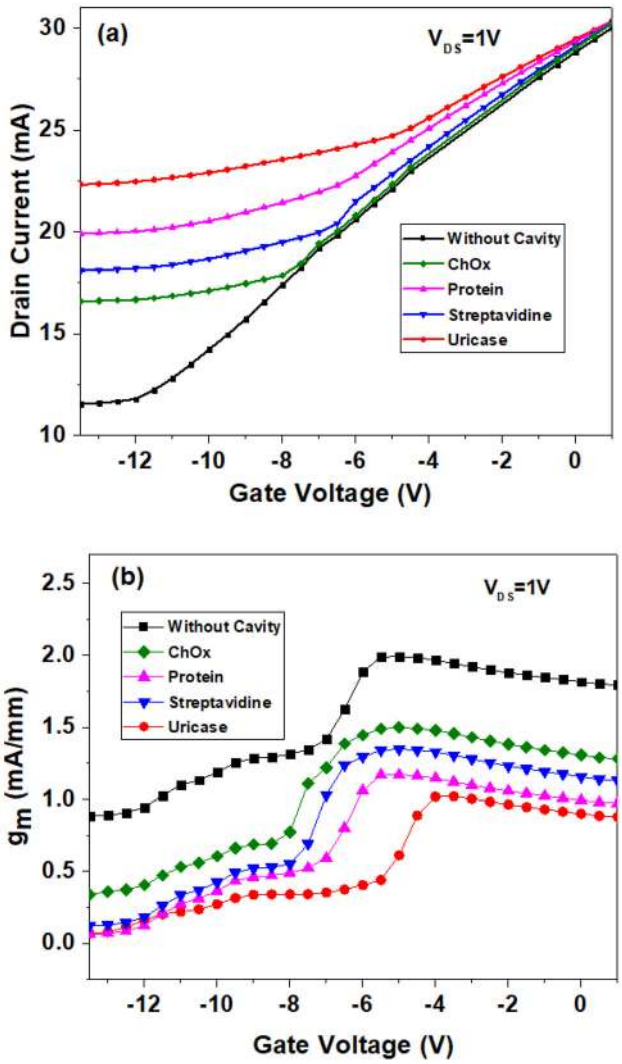

Fig. 5 **a** Output characteristics **b** g_d vs Vd of AlGaN/GaN MOSHEMT with different biomolecules introduced in the cavity

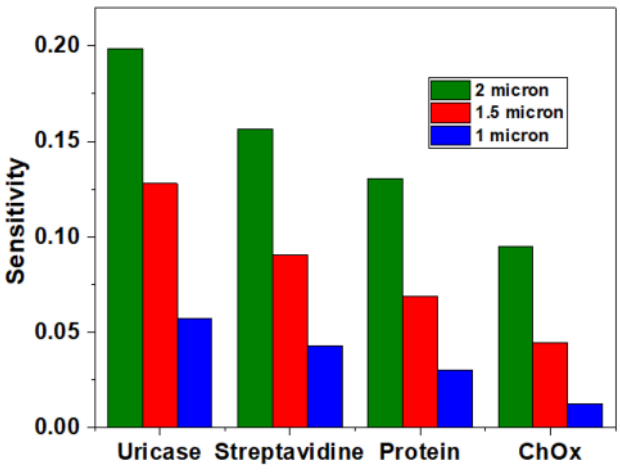

Fig. 6 sensitivity parameter for different biomolecules

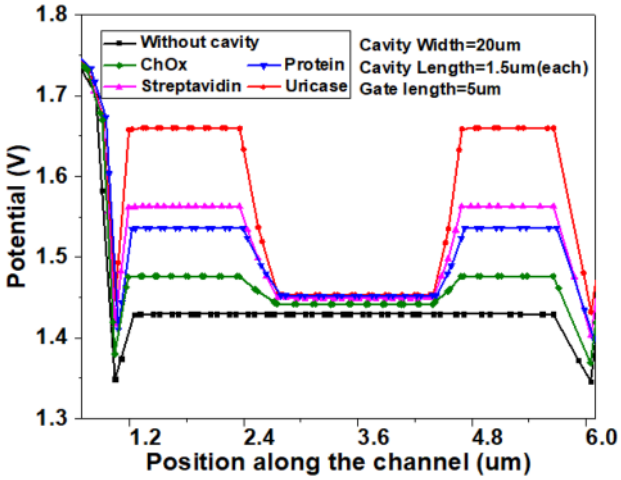

Fig. 7 Channel potential for biomolecules along the channel length

$$I_{D=-q\mu\frac{W_G}{L_G}}\left(\begin{array}{c}\frac{2}{s}\gamma_0\left(n_{drain}^{\frac{5}{s}}-n_{source}^{\frac{5}{s}}\right)+v_{th}\left(n_{drain}-n_{source}\right)\\+\frac{q}{2C_{MOSHEMT}}\left(n_{drain}^2-n_{source}^2\right)\end{array}\right) \quad (5)$$

$\gamma_o = 2.12 \times 10^{-12}$ V $m^{4/3}$ is constant. n_{source} and n_{drain} are charge concentration at source and drain, respectively. W_G is width and L_G is gate length. μ is the low field mobility.

4 Results and discussions

Figure 2 shows the Id-Vd characteristics of the GaN based MOSHEMT having gate length of 5 μm without biomolecule. The core current models used in the simulation are able to reproduce the device characteristics very well. The self-heating effects are not considered in the simulation.

The biomolecules has been introduced in cavities of Wcavity = 20 μm and Lcavity = 1.5 μm on both sides of oxide layer. Figure 3a shows the output characteristics of the device. When biomolecule is introduced in to the cavity, there is enhancement in the carrier concentration in the channel region which causes increase in the drain current. Here Maximum increase of 18 mA in drain current is observed for Uricase. g_d vs Vd plot is shown in Fig. 3b. Since Id-Vd characteristics of the device are changing by presence of biomolecule in the cavity in similar way variation in g_d is also observed.

Table 2 Comparison between MOSHEMT and GAA-JLT [26]

Biomolecule	ChOx	Protein	Streptavidine	Uricase	
Change in current (mA/mm) = current without cavity − current with biomolecule	MOSHEMT (ΔI)	136	224	280	350
	GAA-JLT (ΔI_{off})	0.0033	0.029	0.0538	0.170
Change in threshold voltage (ΔV_{th})	MOSHEMT	4.027	6.614	8.360	10.844
	GAA-JLT	0.038	0.093	0.118	0.150

Figure 4a–e shows the electron concentration contour. Figure 4a shows the no change of concentration when no biomolecule is introduced. As biomolecule is introduced, the more charges gets induced in the channel in the region beneath the cavity. The quantity of charge induced depends on the dielectric constant of the biomolecule as can be seen from Fig. 4b–e. Due to lowest value of dielectric constant in Uricase more charges are induced in the channel that is inferred from the rise of drain current in Fig. 3a.

Transfer characteristics and transconductance are shown in Fig. 5a, b. The positive shift in the threshold voltage is observed when biomolecule is introduced in the cavities. Because the presence of biomolecule induces charges in the channel thus results in the better formation of 2DEG in the channel at lower gate voltage. The Threshold voltage shifted from − 12 V for without biomolecule to − 5.5 V at V_{DS} = 1 V for Uricase. However, with increase of dielectric constant for streptavidin, protein and ChOx negative shift in the voltage is observed as compared to Uricase the due to reduced induced charges. Similarly the change in the transconductance is also observed as shown in Fig. 4b. The maximum transconductance is 2 mA/mm for without biomolecule, 1.5 mA/mm for ChOx, 1.3 mA/mm for Protein, 1.2 mA/mm for streptavidin and 1 mA/mm for Uricase.

Figure 6 shows the sensitivity parameter for different biomolecules. The maximum increase of 0.141 in sensitivity is observed when cavity length is varied from 1 to 2 μm on both each side of the oxide layer. This is due to reason, as cavity length increases, more area of the biomolecule is available to interact with underneath AlGaN functional layer. The maximum increase is observed for Uricase due to its lower dielectric constant. So for high sensitivity applications, the length of the cavity should be more.

Figure 7 shows the potential along the channel at 4 μm below the AlGaN/GaN interface when biomolecule is introduced in the cavity region I&III underneath the gate. Permittivity of the biomolecules is different due to which the potential developed in the channel region changes. Uricase having lowest permittivity is showing potential variation of 10% as compared to 3% for ChOx. The comparison in parameter like on current and threshold voltage for MOSHEMT and GAA-JLT [26] for detection of neutral biomolecule is shown in Table 2. A large change in drain current and threshold voltage of MOSHEMT is observed for all biomolecules.

5 Conclusion

In this paper, the used model accurately predicts the effect of biomolecule species on the performance parameters of GaN based MOSHEMT. There is significant increase in the drain current and change g_d is observed with the addition of biomolecule in the cavity. The electron concentration contour indicates notable increase of electron concentration with addition of biomolecule. The positive shift in the gate threshold voltage, maximum shift of ∼ 54% is observed for Uricase due to lowest dielectric constant. Similarly the notable change in transconductance is also obtained. The sensitivity of the structure increases approximately four times with the increase in the cavity length due to more area of contact of the biomolecule with the underneath functional layer. The rise of 10% in channel potential is viewed when biomolecule (Uricase) is introduced in the cavity. MOSHEMT showed better sensitivity towards drain current and threshold voltage as compared to GAA-JLT. Therefore, it can be concluded that this GaN Based MOSHEMT gives significant change in performance parameters and can be used for biomolecule sensing applications effectively.

Acknowledgements

We would like to thank our guide for motivation, constant guidance and all technical support. Our sincere regards to faculty of Applied Physics

Department, Delhi Technological University, New Delhi.

References

1. J.-Y. Yoon, *Introduction to Biosensors: From Electric Circuits to Immunosensors* (Springer, New York, 2016)
2. A. Kumar, M. Roy, N. Gupta, M.M. Tripathi, R. Chaujar, Dielectric modulated transparent gate thin film transistor for biosensing applications. Mater. Today (2020).
3. F. Ren, J.C. Zolper, *Wide Band Gap Electronic Devices* (World Scientific publication Co. Pte. Ltd, Singapore, 2003)
4. U.K. Mishar, P. Parikh, Y. Wu, AlGaN/GaN HEMTs—an overview of device operation and applications. Proc. IEEE **90**(6), 1022–1031 (2002)
5. O. Ambacher, J. Smart, J. Shealy, N. Weimann, K. Chu, M. Murphy, W. Chaff, L. Eastman, R. Dimitrov, L. Wittmer, M. Stutzmann, W. Rieger, J. Hilsenbeck, Two-dimensional electron gases induced by spontaneous and piezoelectric polarization charges in N- and Ga-face AIGaN/GaN heterostructures. J. Appl. Phys. **85**, 3222–3233 (1999)
6. J. Madan, H. Arora, R. Pandey, R. Chaujar, Analysis of varied dielectrics as surface passivation on AlGaN/GaN HEMT for analog applications. in *International Conference on Wireless Networks & Embedded Systems (WECON-2018)*, p. 15–18, 16–17
7. H. Arora, J. Madan, R. Chaujar, Impact on analog and linearity performance of nanoscale AlGaN/GaN HEMT with variation in surface passivation stack. Mater. Today (2018)
8. T. Aggerstam, S. Lourdudoss, H.H. Radamson, M. Sjödin, Investigation of the interface properties of MOVPE grown AlGaN/GaN high electron mobility transistor (HEMT) structures on sapphire. Thin Solid Films **515**, 705 (2006)
9. V.K. Khanna, Robust HEMT microsensors as pospective successors of MOSFET/ISFET detectots in harsh environment. Front. Sens. **1**(3), 38–48 (2013)
10. M. Stutzmann et al., GaN-based heterostructures for sensor applications. Diamond Relat. Mater. **11**(3), 886–891 (2002)
11. S.U. Schwarz et al., DNA-sensor based on AlGaN/GaN high electron mobility transistor. Phys. Status Solidi A **208**(7), 1626–1629 (2011)
12. N. Kazanskaya et al., FET-based sensors with robust photosensitive polymer membranes for detection of ammonium ions and urea. Biosens. Bioelectron. **11**(3), 253–261 (1996)
13. K.H. Chen, B.S. Kang, H.T. Wang, T.P. Lele, F. Ren, D.M. Dennis, K.J. Linthicum, C-erbB-2 sensing using Al Ga N/Ga N high electron mobility transistors for breast cancer detection. Appl. Phys. Lett. **92**, 192103 (2008). https://doi.org/10.1063/1.2926656
14. N. Kannan, M.J. Kumar, Charge-modulated underlap I-MOS transistor as a label-free biosensor: a simulation study. IEEE Trans. Electron Devices **62**(8), 2645–2651 (2015)
15. Y. Chen et al., Field-effect transistor biosensor for rapid detection of Ebola antigen. Sci. Rep. **7**(1), 1–8 (2017)
16. G.H. Chung, T.A. Vuong, H. Kim, Demonstration of hydrogen sensing operation of AlGaN/GaN HEMT gas sensors in extreme environment. Physics **12**, 83–84 (2019). https://doi.org/10.1016/j.rinp.2018.11.064
17. W.D. Hu, X.S. Chen, Z.J. Quan, X.M. Zhang, Y. Huang, C.S. Xia, W. Lu, P.D. Ye, Simulation and optimization of GaN-based metal-oxide-semiconductor high-electronmobility-transistor using field-dependent drift velocity model. J. Appl. Phys. **102**, 034502 (2007). https://doi.org/10.1063/1.2764206
18. G. Seo, G. Lee, J.-O. Lee, B.T. Kim, E.C. Park, S.I. Kim, Rapid detection of COVID-19 causative virus (SARS-CoV-2) in human nasopharyngeal swab specimens using field-effect transistor based biosensor. Am. Chem. Soc. **14**(4), 5135–5142 (2020). https://doi.org/10.1021/acsnano.0c02823
19. T. Wang, L. Lou, C. Lee, A junctionless gate-all-around silicon nanowire FET of high linearity and its potential applications. IEEE Electron Devices Lett. **34**(4), 478–480 (2013)
20. L. Xiang, Z. Chen, N. Shen, N. Singh, K. Banerjee, G.Q. Lo, D.L. Knong, Vertically stacked and independently controlled twin-gate MOSFETs on a single silicon nanowire. IEEE Electron Devices Lett. **32**(11), 1492–1494 (2011)
21. S. Taking, D. MacFarlane, E. Wasige, AlN/GaN-based MOS-HEMT technology: processing and device results. Act. Passiv. Electron. Compon. (2011). https://doi.org/10.1155/2011/821305
22. K. Han, L. Zhu, GaN MOSHEMT employing HfO2 as a gate dielectric with partially etched barrier. Semicond. Sci. Technol. **32**(9), 095004 (2017)
23. I.M. Hyungsoon, X.-J. Huang, B. Gu, Y.-K. Choi, A dielectricmodulated field-effect transistor for biosensing. Nat. Nanotechnol. **2**, 430–434 (2007)
24. Y. Yuan-Zheng, H. Yue, F. Qian, N. Jin-Yu, GaN MOS HEMT using Ultra thin Al_2O_3 dielectric grown by atomic layer deposition. Chin. Phys. Lett. **24**(8), 2419 (2007)
25. F.M. Yigletu, S. Khandelwal, T.A. Fjeldly, B. Iñiguez, Compact charge-based physical models for current and capacitances in AlGaN/GaN HEMTs. IEEE Trans. Electron Devices **60**(11), 3746–3752 (2013)
26. Y. Pratap, M. Kumar, S. Kabra, S. Haldar, R.S. Gupta, M. Gupta, Analytical modeling of gate-all-around junctionless transistor based biosensors for detection of neutral biomolecule species. J. Comput. Electron. **17**, 288–296 (2018)